Journal of Fluorescence, Vol. 11, No. 3, September 2001 (© 2001)

Ultrasensitive Microscopy of the Plasma Membrane of Living Cells

G. J. Schütz,[1,2] M. Sonnleitner,[1] and H. Schindler[1]

The view of the plasma membrane of biological cells was dramatically changed due to the discovery of lipid domains. Initially found as structurally distinct areas characterized by a specific protein content, the concept of lipid domains was rapidly taken over as a new scheme for explaining membrane targeted cellular processes. In this review, we discuss the capabilities of imaging methodologies to study lipid domains and their contributions to the current model of the cellular plasma membrane.

KEY WORDS: Lipid microdomains; cell membrane; single molecule microscopy; fluorescence microscopy.

INTRODUCTION

The main function of the cellular plasma membrane is generally seen to be to act as a barrier for ions and macromolecules, preventing both unhindered access to the interior of the cell and uncontrolled loss to the exterior. In this view, lipids build up mainly the separating matrix, in which embedded membrane proteins allow the controlled exchange of substances or transduction of signals between outside and inside. These processes often require a concerted action of different types of proteins, which are transiently assembled in complexes over the plasma membrane. The assembly and disassembly of such complexes are a major regulatory principle for cellular function, which allows the sharing of the same molecules for different processes. Fast reassembly upon an external trigger, however, requires the close proximity of the involved protein molecules. Therefore it would be highly favorable for a cell to confine certain proteins physically to distinct zones within the plasma membrane, which serve as signaling platforms. These confinement zones were postulated long before they were actually seen [1]. Striking evidence for the existence of domains within the plasma membrane of cells came first from biochemical extraction of the membrane, with subsequent sucrose density-gradient centrifugation, which allowed the qualitative distinguishment of a distinct part of the plasma membrane which is not soluble in mild detergent [2]. Careful investigation of this so-called detergent-resistant membranes (DRM) further yielded its protein content, which was found to be consistently different from that of the remaining fractions of the membrane [3,4]. Most proteins involved in signaling were found to be enriched in these DRMs [5].

The physical origin and *in vivo* counterpart of DRMs are still under debate. The detergent insolubility is most likely mediated by self-interaction between glycosphingolipids [6]. In addition, a distinct set of lipids was found to be enriched in DRMs [2], such as sphingolipids [7], fully saturated fatty acids [8], and cholesterol [2]. Following the lipid content, different terminologies emerged for plasma membrane domains, such as sphingolipid–cholesterol microdomains [9], ganglioside-enriched membranes (GEMs) [10], detergent-insoluble glycosphingolipid-enriched domains (DIGs) [11], and lipid rafts [6]. Investigation of detergent-resistant liposomes allowed the characterization of the phase state of DRMs as an ordered liquid phase [6,12]. This ordered environment highly

[1] Institute for Biophysics, University of Linz, Altenbergerstr. 69, A-4040 Linz, Austria.
[2] To whom correspondence should be addressed. Fax: +43-732-2468-9280. E-mail: gerhard.schuetz@jk.uni-linz.ac.at

1053-0509/01/0900-0177$19.50/0

enhances the partitioning of those proteins, which are linked to saturated acyl chains, such as glycosylphosphatidylinositol (GPI)-anchored proteins or proteins acylated with myristate or palmitate [13,14].

Modulation of the lipid domains can be achieved in two ways. First, The domain itself can be affected by changing the cholesterol content of the plasma membrane. Depletion of membrane cholesterol using methyl-β-cyclodextrin leads to disruption of domains [15], thereby making cholesterol a candidate for controlling domain formation [16]. In addition to cholesterol, ceramides as precursors of sphingolipids were discussed as possible modulators for lipid raft formation in the plasma membrane [17,18]. Second, a certain protein can be modified. Palmitoylation and/or myristoylation are common principles for targeting enzymes to the plasma membrane and thence to specific domains [13]. This process is reversible, allowing the rapid assembly and disassembly of signaling units.

Beside their initial importance for the discovery of plasma membrane domains, detergent extraction methods are still widely used to study the targeting of membrane proteins, either to rafts or to the remaining part of the plasma membrane, thereby setting a widely accepted standard for terminology. However, there are major limitations to this methodology. First, artifacts due to relocalization of proteins during detergent extraction have been reported [19,20]. Second, to avoid degradation processes, solubilization of cells has to be performed at low temperatures, which might influence domain properties [21,22]. And, finally, no information is obtained on the actual size, shape, and dynamics of domains in living cells. In this review, we describe methodologies capable of imaging domains within the plasma membrane of intact cells, and we discuss the outcome of these studies in comparison to biochemical results.

METHODOLOGIES

The most common imaging techniques in cell biology are based on fluorescence microscopy. Typically, membrane proteins are specifically addressed using either fluorescence-labeled ligands, such as antibodies, or fusion constructs of proteins with green fluorescent protein or one of its mutants [23]. In some studies, GPI-anchored proteins were labeled directly before insertion into the plasma membrane [24,25]. For studying lipids, the most commonly used reagent is fluorescence-labeled cholera toxin, which stains specifically the ganglioside GM1 [26]. In addition, fluorescence-labeled saturated phospholipids were used to image individual microdomains directly in living cells [27].

The principal advantage of fluorescence microscopy over static imaging methods is its applicability to living cells, resolving dynamical properties down to imaging molecular processes. Its limitation relates to the resolution of light microscopy, which is set principally by the diffraction limit of a few hundred nanometers. The resolution can be substantially enhanced, to ~50 nm, using scanning techniques, such as near-field microscopy, or techniques for the study of individual molecules, such as single-particle tracking or single-dye tracing. Combination with nonoptical methods such as electron microscopy and atomic force microscopy provided added value. An overview of the basic parameters characterizing the techniques discussed is given in Table I.

Confocal/Two-Photon Laser Scanning Microscopy (CLSM/TPLSM)

CLSM is currently the most commonly applied technique for studying distributions of proteins and lipids within the plasma membrane. The technique itself is based on scanning a focused laser beam over the sample and detecting the emitted fluorescence signal using a photodiode. The basic advantage over conventional microscopy arises from the use of a pinhole before the detector, which effectively reduces the detection volume. Therefore, only light emitted within the focal plane can reach the detector; signal from adjacent planes is effectively blocked. This enhances mainly the resolution along the optical axis to ~0.5λ, with λ the excitation wavelength [28]. A similar effect is achieved using the principle of two-photon excitation. Ultrashort light pulses are used for excitation of chromophores by simultaneous absorption of two photons with half the transition energy

Table I. Basic Parameters of the Techniques Discussed

Technique(s)	Applied to living cells	Lateral resolution	Time resolution[a]
CLSM, TPLSM	Yes	~250 nm	100 s
FRET	Yes	5 nm	—
SNOM	No	80 nm	600 s
SPT	Yes	10 nm[b]	<1 ms
SDT	Yes	40 nm[b]	10 ms
EM	No	1 nm	—
AFM	Yes	10 nm	100 s

[a] The time required to image a 10 × 10-μm area at the lateral resolution specified (double oversampling).

[b] Referred to the single-molecule resolution, not to the diffraction limit (see text).

[29,30]. The resulting quadratic dependence of the fluorescence signal on the illumination intensity enhances largely the resolution along the optical axis [31]. An interesting side effect of this technique is the possibility to excite different fluorophores simultaneously with the same excitation wavelength due to broad two-photon absorption spectra [32]. This can be implemented most easily in conventional TPLSM setups, thereby enabling simultaneous two-color imaging [33].

CLSM was applied to study the distribution of various fluorescence-labeled proteins and lipids within the plasma membrane of fixed cells, which allowed the discrimination of plasma membrane domains and characterization of their protein content. Distinct localization within membrane domains has been observed for GPI-anchored proteins such as CD48 [15] and CD59 [25], but also for transmembrane proteins such as the IgE receptor [34], CD4 [35], CD40 [36], the IL-2 receptor [15], the chemokine CCR5 receptor [37], the transmembrane phosphoprotein Cbp [38], and the Cbl–CAP complex involved in glucose uptake [39]. To clarify the underlying structure for protein confinement, cross-correlation of the distributions of different proteins and/or lipids was performed using two excitation wavelengths for two fluorescent labels. Thereby it was shown that the ganglioside GM1 colocalizes with the IgE receptor [34], CD40 [36], and the CCR5 receptor [37]. Two distinct sets of domains were observed for the two transmembrane proteins PLAP and prominin [40]. In addition to the characterization of domain properties, several studies have investigated the redistribution of signaling molecules or whole domains upon a stimulus [40–44].

In comparison to detergent extraction methods, CLSM allows measurements on intact cells. This yields a three-dimensional map of the protein density of a cell, thereby also showing the lateral extension of domains. Still, calculations of domain sizes are estimations with a great uncertainty, since the numbers are of the order of the lateral resolution of confocal microscopy, ranging, e.g., between 600 and 800 nm for the IL-2 receptor [15]. Especially, substructures within these domains cannot be resolved. A second drawback of this methodology is the limited time resolution due to scanning. Assuming an image size of 10×10 μm, a lateral step size for scanning at optimum system settings of $\sim$0.1 μm [45], and an acquisition time for one pixel of $\sim$10 ms, the delay between two consecutive images of the same area is of the order of 100 s. For such slow frame rates, the residual mobility of domains and whole cells would blur the image. Therefore, in most applications cells were fixed before imaging. Efforts were made to improve the time resolution of CLSM and TPLSM by scanning multiple laser beams over the sample [46–48]. In addition, utilizing ultrasensitive detectors such as single-molecule detection methods would still allow a significant signal-to-background ratio at even shorter illumination times, thereby increasing the possible frame rate up to 1 frame/10 s, which would allow the unraveling of dynamic processes of individual domains, which typically proceed in a seconds time frame [27].

Figure 1 shows two TPLSM images of the top surface of a living TSA cell double-labeled with cholera toxin–FITC for staining GM1 domains (green channel) and DPPE–TMR (red channel). The images were taken with a time delay of 13.4 s. Clearly, one can observe two distinct domains enriched in both GM1 and DPPE. The relatively fast scanning speed allows the resolution of domain mobility, thereby making this method well suited for imaging shifts in the position as well as fluctuations in the shape and size of individual plasma membrane domains.

Fluorescence Resonance Energy Transfer (FRET) Microscopy

FRET occurs when two dye molecules, a donor and an acceptor with significant spectral overlap, are in close proximity, typically $<$5 nm [49]. In this case, excitation of the donor yields a fluorescence signal characteristic for the acceptor. The transfer efficiency itself is highly dependent on the distance between donor and acceptor, making FRET a sensitive tool to study colocalization between two different types of molecules on length scales of several nanometers. The second type of experiments utilizes FRET between the same type of molecules, thereby obtaining information on the local protein density, again in a sensitive region of a few nanometers.

Both strategies have been applied to investigate plasma membrane domains. Colocalization of HLA class I and class II was confirmed via FRET between two differently labeled molecules [50]; in a very elaborate study, lipopolysaccharide- and ceramide-induced clustering of various CD receptors within rafts in monocytes was investigated in the context of new descriptions of the signaling pathway relevant for sepsis or atherogenesis [51]. FRET between the same type of molecules can be utilized in an elegant way for determination of clustering on subwavelength scales. By comparing the average number of molecules per pixel, as given by the intensity, and the local protein density, given by the FRET signal, the distribution of the proteins within one pixel can be estimated. Using this approach, the existence and size of clusters have been studied for GPI-anchored proteins; while one study yielded no significant evidence for clus-

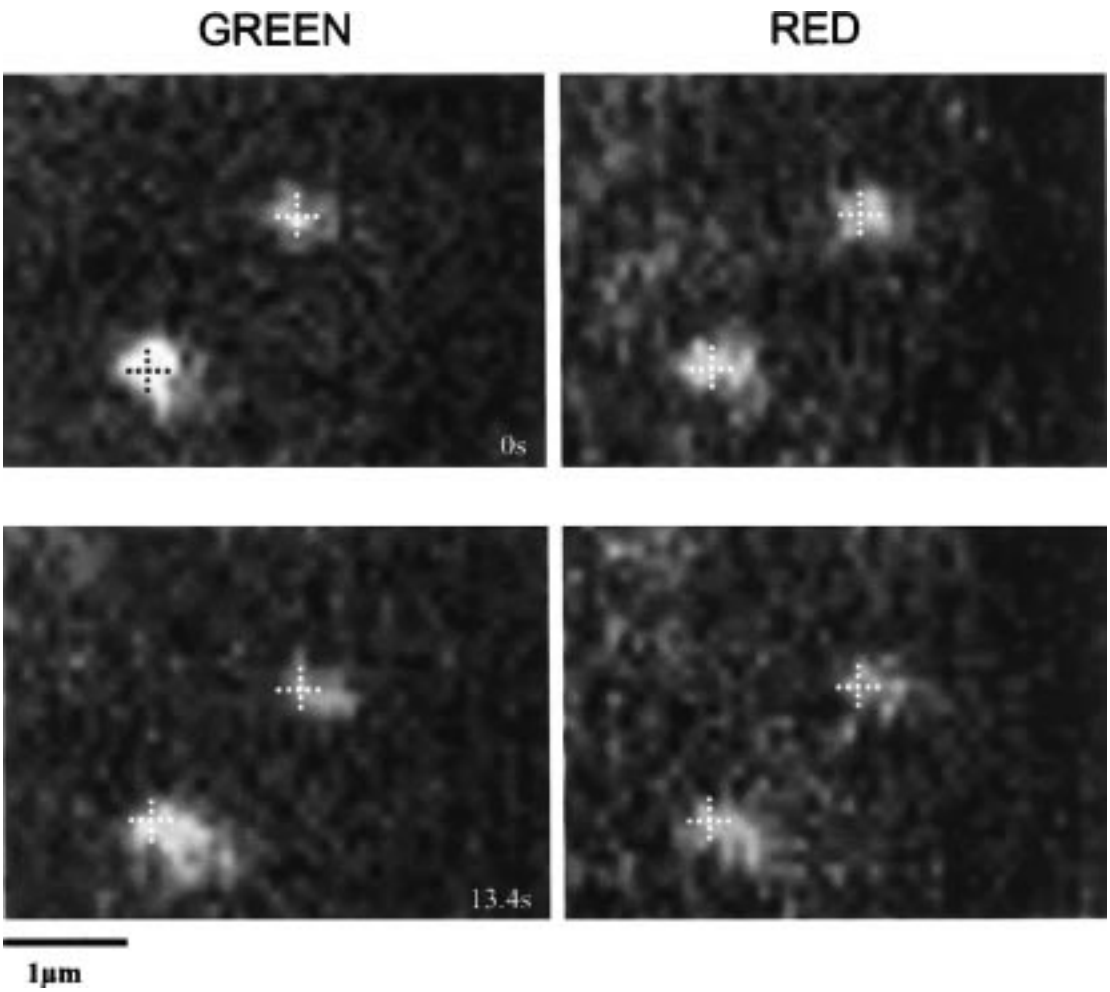

Fig. 1. Two consecutive TPLSM-images of the top membrane of a tsA201 cell showing two lipid domains moving within the plasma membrane. The domains contain GM1 labeled with Choleratoxin-FITC (green channel), and TMR-DPPE (red channel). GM1 and DPPE domains were colocalized within the detection limit of ~100 nm. For clarity, the position of both domains in the first observation was indicated by a white cross; a movement of the domains within the time-lag of 13.4 s is clearly visible. Cells were incubated for 20 minutes with 1.25 µg/ml FITC-labeled Choleratoxin (ChT-subunit B) and 30 µg/ml of vesicles containing a mixture of TMR labeled DPPE and unlabeled POPC with a ratio of 10^{-3} [27]. After incubation, the top membrane of a cell was scanned with a dwell time of 1 ms and a stepwidth of 0.1 µm using a Two Photon Laser system with a mean power of 6 mW at a wavelength of 800 nm, thereby exciting both fluorophores, FITC and TMR, simultaneously. A dichroic mirror in the emission path was used to split the fluorescence of the individual fluorophores, which is detected by two avalanche photodiodes.

tering [52], in a second study domains were detected with a size estimated as 70 nm [53].

FRET itself is not an imaging method, thus there is no direct access to the principally high resolution of the method, yielding the interpretation of the results highly model dependent. However, the transfer efficiency can be obtained in parallel during experiments performed with all types of fluorescence microscopy, e.g., by using two detection channels, thereby enhancing the information content of a standard image.

Scanning Near-Field Optical Microscopy (SNOM)

This technique is based on scanning a very small light source, typically a glass fiber with a diameter much smaller than the wavelength of the excitation light, very close (in the near-field) to the specimen (see, e.g., Ref. 54). SNOM is a proximity method (in application to cells it is restricted to cell surfaces) with a high lateral resolution, down to 80 nm [55], and a high background rejection due to the very small excitation volume. Still,

there is only a small amount of literature available for applications of SNOM to cellular systems, due mainly to technical problems [56], especially high interaction forces between the fiber tip and the cell membrane [54], which would lead to disruption of the plasma membrane of a living cell. To avoid this, studies of plasma membrane domains with SNOM have been restricted to fixed cells. There, clustering of HLA class I molecules to domains of 300–600 nm was determined [57]. SNOM was also utilized for studying colocalization of differently colored molecules at a resolution of ~100 nm, exemplified for the MESA/protein4.1 pair on erythrocytes [58].

Single-Particle Tracking (SPT)

SPT employs large particles (colloidal gold particles, heavily fluorescence-labeled polystyrene beads, or biomacromolecules) for the tracking of molecules at cell surfaces to which the particles are linked ([59]; for a review see Ref. 60). The high signal of these particles, even at a low illumination intensity, allows for continuous tracking of the particles with nanometer precision on a millimeter time scale [61–64]. Due to the high positional accuracy of SPT, structural elements in plasma membranes of living cells can clearly be resolved as barriers to the diffusional mobility of the probe molecules. Such studies led to a classification of molecular motions in cell membranes into different modes of motion, which allowed for separate analysis of subpopulations of molecules undergoing free Brownian motion, confined diffusion, anomalous diffusion, directed motion, or binding to immobile structures [63,65–68].

In particular, SPT has brought considerable new insights as a tool to study compartmentalization of cell surfaces [64,69–73]. Restrictions of lateral mobility have been observed for proteins such as Band 3 [74], E-cadherin [75], NCAM (neural cell adhesion molecule [68]), and the transferrin receptor [65].

The basic advantage of SPT lies in its high resolution, which allows the determination of the size of subwavelength confinement zones. Practically, one can follow directly the path of single molecules moving over the plasma membrane, thereby getting additional information on the time scale of confinement. The problem in doing so arises from the highly stochastic nature of such a random walk. Especially, in the case of weak confinement, the trajectory does not cover the whole domain, rendering the determination of actual domain sizes from individual trajectories difficult [76]. In addition, the residual mobility of the domains themselves [27] affects the trajectory of the confined molecule studied, yielding systematical deviations to larger domain sizes. Another disadvantage of SPT as a method to study submicron structures of membranes is the use of large marker particles. Interaction with the extracellular matrix [77] or cross-linking [72] may be overcome with smaller labels, down to the ultimate limit of a single molecule, at the expense of a lower signal-to-noise ratio. A promising intermediate step might be the use of phycobiliproteins [78–81] or semiconducting nanoparticles [82,83] with a size of several nanometers. However, the photophysical characterization of nanoparticles needs further investigation.

Single-Dye Tracing (SDT)

SDT utilizes conventional wide-field epifluorescence microscopy at a sensitivity which permits imaging of single mobile fluorophores within the image plane at a millisecond time resolution (for reviews, see Refs. 84 and 85). In essence, SDT advances SPT to the single-dye marker level, with further advantages based on observing a single quantum system. It allows the study of the motion of individual molecules [86], with additional information on stoichiometry [87], orientation [88,89], and colocalization between different molecules [90]. In the following, we add some considerations on the principles of single-molecule microscopy in general, specifically with regard to its applicability to living cells.

The image of a single-dye molecule is represented by a diffraction-limited spot on the camera. An automatic fitting algorithm allows the determination of the position of the molecule to an accuracy of ~50 nm. To allow unambiguous single-molecule identification, the concentration of molecules has to be much lower than 1/resel (resel = resolution element of the microscope). Assuming an equal distribution of molecules on a surface, the probability that the distance to the nearest neighbor is larger than the size of the diffraction-limited spot of $r = 500$ nm is given by $F_{nn}(r) = \exp(-r^2\pi n)$ [91], with n the concentration of dye molecules. For a certainty $F > 95\%$, n has to be less than 1 molecules/15 μm^2. To trace mobile molecules in consecutive images, the concentration has to be reduced further. Let us assume that molecule A moves a distance r_D within the time lag t between two consecutive observations. Let us assume further that this mobility is based on lateral diffusion with diffusion constant D. The criterion for unambiguous tracing of molecule A is then based on the probability that r_D is smaller than the distance of the nearest neighbor, r_{nn}. This probability can be calculated as $p(r_D < r_{nn}) = \int_0^\infty F_D(r)\, f_{nn}(r)\, dr$, where $f_{nn} = \frac{dF_{nn}}{dr_{nn}}$ denotes the probability density for the distance to the nearest neighbor, and

$F_D(R) = \int_0^R \frac{r}{2Dt} \exp\left(-\frac{r^2}{4Dt}\right) dr$ the probability distribution for diffusional motion. $p\,(r_D < r_{nn}) > 95\%$ is fulfilled for surface densities $n < 1$ molecule/25 μm^2, assuming a common diffusion constant of lipids of $D = 1$ $\mu m^2/s$ and a typical time lag of 100 ms. This means, for unambiguous tracing at a level of certainty of 95%, that not more than ~12 fluorescence-labeled molecules should be located within the plasma membrane of a typical small cell, with a diameter of ~5 μm. Therefore, single-molecule methods are best suited for the investigation of low-abundance proteins. Studying biomolecules with a higher abundance requires underlabeling.

To achieve single-molecule sensitivity, the transmission efficiencies of all optical elements in the detection path have to be maximized. In general, the overall detection efficiency, η, can be separated into three factors: the efficiency of the microscope objective, η_O, of optical filters, η_F, and of the detector, η_D. Typical values are $\eta_O \sim 30\%$ for an oil immersion objective with NA = 1.4, $\eta_F \sim 50\%$, and $\eta_D \sim 80\%$, yielding $\eta \sim 12\%$. Obviously, the limiting factor is the objective, which collects only a minor fraction of all emitted photons due to the limited collection angle set by the numerical aperture. At optimized settings, such systems allow one to obtain images of single dye molecules in synthetic environments at a high signal-to-background ratio, ~30. Besides the high detection efficiencies, this is related mainly to the low noise characteristics of liquid nitrogen-cooled CCD cameras. Thus, about 150 photons can be detected from a single molecule within brief illuminations of 5 ms, short enough to neglect any mobility of the biomolecule during illumination.

The application of single-molecule methodologies to living cells, however, yielded major difficulties due to the substantial cellular background fluorescence, due mainly to NADH and FAD [92–94]. Still, several groups have successfully proven single-molecule detection in living cells, by carefully selecting the fluorophore and/or a cell line with low autofluorescence [27,95–97]. Two sources of fluorescence background have to be considered in cells: first, the *nonhomogenous background*, due to autofluorescent diffraction-limited objects containing high amounts of NADH and FAD, such as mitochondria [98]. At excitation wavelengths below ~550 nm, these features can easily be discriminated from single dye molecules by their higher fluorescence intensity. At long wavelength excitations, the fluorescence intensities become comparable to the values expected for single fluorophores. In this case, mitochondria can be discriminated by their distinct photobleaching behavior: during prolonged excitation, the fluorescence signal slowly vanishes due to the small extinction coefficient of FAD, whereas single molecules show one-step photobleaching. Second, the *homogenous background* has to be considered, which comprises either out-of-focus fluorescence from small objects or signal arising from autofluorescent molecules dispersed in the cytoplasm. Again, the background decreases with increasing wavelength due to low absorption of biological material above 550 nm, making long-wavelength excitation best suited for single-molecule studies in cells. However, the homogenous background is not a systematic limitation of the methodology itself, since it reduces only the positional accuracy [99]. Still, an accuracy of ~40 nm for assigning the position of a single molecule within the plasma membrane of a living cell can be achieved routinely [95].

We utilized SDT to study the lateral diffusion of fluorescence-labeled lipids with unsaturated or fully saturated acyl chains, thereby affecting the affinity to microdomains within the plasma membrane (Fig. 2; see also Ref. 27). Fluorescence-labeled probe lipids were introduced into the plasma membrane by incubating the cells with vesicles made of POPC as a host for the respective probe lipid at a ratio of $\sim 1{:}10^{-3}$. This energetically highly unfavorable procedure allows the adjustment of the final amount of probe lipids in the plasma membrane to concentrations of ~1/100 μm^2, which is sufficiently low for unambiguous identification of single-molecule trajectories. These trajectories of individual lipid molecules show directly whether a molecule diffuses freely within the plasma membrane or whether it has been confined to a certain domain. In addition to a qualitative statement, this approach allows one to calculate the domain size (~700 nm) and the residual mobility of the lipid molecule within the domain ($D = 0.6$ $\mu m^2/s$). Similarly to SPT, SDT allows the determination of such properties on length scales significantly below the diffraction limit of light microscopy. Furthermore, by increasing the number of fluorescence-labeled lipids in the membrane, it was possible to observe individual domains directly with a millisecond time resolution. Domains were mainly immobilized on the plasma membrane, but on occasion we observed directed transport to a different position within the membrane.

The basic limitation of single-molecule microscopy in general is related to the limited number of observations of a single fluorophore possible before it photobleaches permanently [100], restricting the length of single-molecule trajectories to a few tens of images, depending on the fluorophore used and the signal-to-background ratio.

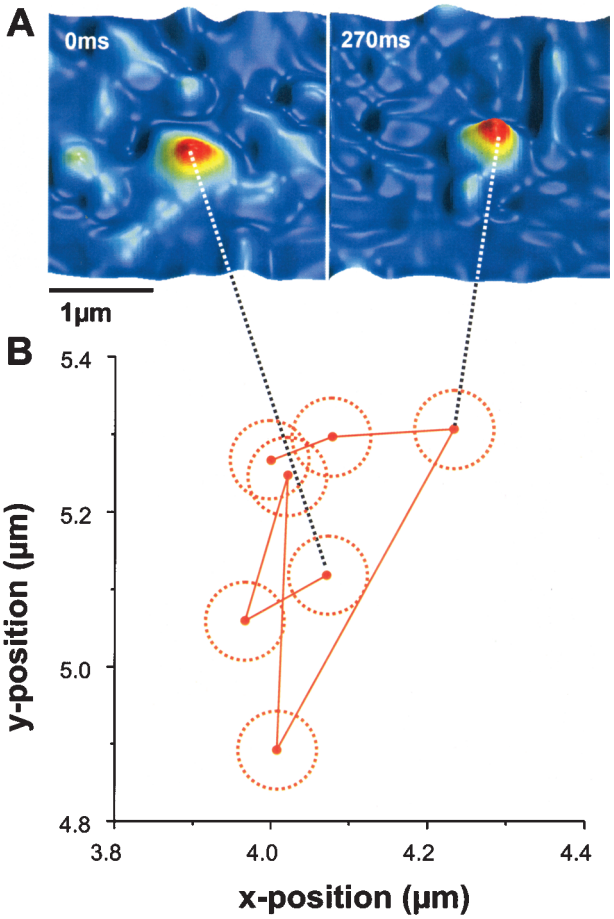

Fig. 2. (**A**) Two successive images of a single Cy5-labeled lipid (DOPE) within the plasma membrane of a smooth muscle cell at a time lag of 270 ms. Fluorescence-labeled lipids were introduced via lipid vesicles containing a mixture of Cy5-labeled DOPE and unlabeled POPC at a ratio of 10^{-3} [27]. The lipid moves freely within the membrane, with a diffusion constant of ~0.3 $\mu m^2/s$ [27]. The high positional accuracy of ~40 nm allows us to analyze these trajectories on length scales below the diffraction limit of light microscopy. (**B**) The full trajectory recorded for this molecule. The circles indicate the positional accuracy of each position measured. This trajectory hardly exceeds the size of a diffraction-limited spot, thereby illustrating the principle advantage of single-molecule techniques: the possibility of studying mobility on length scales beyond the diffraction limit of light microscopy.

Electron Microscopy (EM)

EM on immunogold-labeled proteins within the plasma membrane gives the best resolution of all present imaging methodologies and allows one to observe even substructural features of domains. So the tyrosine kinases Lyn and Syk were found to prefer different regions close to the cross-linked FcεRI, with Syk being recruited to large receptor clusters and Lyn in distinct strings and clusters in close proximity [101]. In addition, EM was used to discriminate between caveolae and domains enriched in GPI-anchored proteins [102]. Typically, EM was used to confirm further localization or colocalization within plasma membrane domains using ultrathin slices [15,26,35,43]. The only drawback relates to the massive preparative treatment of cells, which might affect domain properties. In addition, no three-dimensional information can be obtained.

Atomic Force Microscopy (AFM)

AFM is a technique with most captivating potential to yield images of living cells at nanometer resolution. Significant advances in technological developments in the last few years have made it possible to image cellular structures, monitor slow processes in cells in real time, and study micromechanical properties [103,104]. Especially, the development of methods capable of resolving molecular interactions between the modified AFM tip and the sample on the single-molecule level [105–108] offers the possibility of directly localizing regions with a high density of a certain protein at a resolution of ~10 nm. On model membranes, significant substructures within lipid domains in a ternary mixture of phospholipids and the ganglioside GMI has already been shown [109]. Similar studies on cells are still missing, due mainly to the higher flexibility of a cell membrane, which significantly reduces the lateral resolution of the images. Up to now, only studies on fixed cells have yielded new insights into domain properties, e.g., into the interaction of DRMs with the cytoskeleton [110].

While its unbeaten high resolution makes AFM the most appropriate method for studying the lateral extension of domains on living cells, there are basic limitations to be considered. First, AFM is restricted to the top surface, which limits its applicability to restricted parts of a cell membrane. Second, AFM is a scanning technique, with a low time resolution compared to imaging techniques. Especially, in the case of the residual mobility of domains, this fact leads to blurring of the image, similarly to CLSM. The time resolution might be significantly enhanced using small-cantilever force microscopy, which was recently developed for much faster scanning rates [111].

Other Techniques

There are a few other techniques which have been applied recently for obtaining information on membrane domains. One relies on the change in the spectral properties of pyrene upon clustering due to excimer formation, which was utilized to study cluster formation of pyrene-

labeled GM1 [112]. Significant changes in the GM1 content within domains were observed upon the addition of protein kinase C, yielding one of the first direct observations of an induced change in the lipid content of plasma membrane domains.

The second technique is based on monitoring the energy profile experienced by a 200-nm fluorescent latex sphere within a laser optical trap. Changes in this energy profile due to binding of the latex sphere to a membrane protein can be utilized to estimate the viscosity of the surrounding membrane and thereby the size of the associated structure [113].

THE EMERGING VIEW OF PLASMA MEMBRANE ORGANIZATION

Advances in the development of imaging methodology allowed a refined view of the lateral heterogeneities of the cellular plasma membrane. In combination with results from biochemical assays, there is a wealth of new information on the functional role and the structural basis of membrane domains, excellently reviewed in Refs. 114 and 115. For the first time, imaging methodologies permit direct visualization of membrane domains, with detailed characterization beyond merely proving the existence of such domains:

- Plasma membrane domains are dynamic structures regarding shape, motion, and occurrence.
- Domains often appear as dynamic assemblies of smaller units of about 50-nm size.
- Domains can carry different sets of proteins and therefore different functions, whereby the relation between the domain function and its dynamics is still to be disclosed.
- There are distinct types of domains confining different proteins.
- Domains contain substructures: The large variability in domains sizes estimated from results obtained with different imaging methodologies makes it highly plausible that small distinct units with a size of about 50 nm coalesce into large structures with extensions of up to 1 μm.

There are many reports on translocation of proteins into and out of domains as assayed on the level of DRMs. Still, little is known about the actual function of thus-analyzed domains in membrane-associated biological processes. Especially, the relationship between different types of domains remains unclear. It seems that confinement of proteins is only one effect of domains; additional sorting into different confinement zones might be required to separate different signaling platforms. The new image of the plasma membrane emerges as a highly organized pattern of different types of domains, sharing some of its proteins, but efficiently separating others, and being transported through the fluid matrix of the plasma membrane. Ultrasensitive microscopy techniques provide a promising platform to unravel this emerging view in the near-future.

ACKNOWLEDGMENTS

This work was supported by the Austrian Federal Ministry of Science and Transport (Projects GZ 200.025/3-Pr/4/98 and GZ 200.027/3-III/2a/98) and by the Austrian Research Funds (P12803-MED and P12097-PHY).

REFERENCES

1. J. D. Morrisett *et al.* (1975) *J. Biol. Chem.* **250**, 6969–6976.
2. D. A. Brown and J. K. Rose (1992) *Cell* **68**, 533–544.
3. M. P. Lisanti *et al.* (1994) *J. Cell Biol.* **126**, 111–126.
4. K. A. Melkonian *et al.* (1995) *Biochemistry* **34**, 16161–16170.
5. V. Horejsi *et al.* (1999) *Immunol. Today* **20**, 356–361.
6. K. Simons and E. Ikonen (1997) *Nature* **387**, 569–572.
7. R. E. Brown (1998) *J. Cell Sci.* **111**, 1–9.
8. R. Schroeder *et al.* (1994) *Proc. Natl. Acad. Sci. USA* **91**, 12130–12134.
9. A. Rietveld and K. Simons (1998) *Biochim. Biophys. Acta* **1376**, 467–479.
10. A. Terzhagi *et al.* (1993) *Biochemistry* **32**, 9722–9725.
11. R. G. Parton and K. Simons (1995) *Science* **269**, 1398–1399.
12. D. A. Brown and E. London (1998) *J. Membr. Biol.* **164**, 103–114.
13. M. D. Resh (1999) *Biochim. Biophys. Acta* **1451**, 1–6.
14. D. A. Brown and E. London (1998) *Annu. Rev. Cell Dev. Biol.* **14**, 111–136.
15. G. Vereb *et al.* (2000) *Proc. Natl. Acad. Sci. USA* **97**, 6013–6018.
16. D. Hoekstra and S. C. D. van Ijzendoorn (2000) *Curr. Opin. Cell Biol.* **12**, 496–502.
17. K. Venkataraman and A. H. Futerman (2000) *Trends Cell Biol.* **10**, 408–412.
18. E. E. Prieschl and T. Baumrucker (2000) *Immunol. Today* **21**, 555–560.
19. T. V. Kurzchalia *et al.* (1995) *Trends Cell Biol.* **5**, 187–189.
20. M. Pierce and H. Metzger (2000) *J. Biol. Chem.* **275**, 34976–34982.
21. X.-M. Li *et al.* (2000) *Biophys. J.* **78**, 1921–1931.
22. E. London and D. A. Brown (2000) *Biochim. Biophys. Acta* **1508**, 182–195.
23. R. Y. Tsien (1998) *Annu. Rev. Biochem.* **67**, 509–544.
24. F. Zhang *et al.* (1992) *Proc. Natl. Acad. Sci. USA* **89**, 5231–5235.
25. C. van den Berg *et al.* (1995) *J. Cell Biol.* **131**, 669–677.
26. T. Harder *et al.* (1998) *J. Cell Biol.* **141**, 929–942.
27. G. J. Schütz *et al.* (2000) *EMBO J.* **19**, 892–901.
28. G. S. Kino (1995) in J. B. Pawley (Ed.), *Handbook of Biolocical Confocal Microscopy, Plenum Press*, New York, pp. 155–165.
29. M. Göppert-Mayer (1931) *Ann. Phys.* **9**, 273–295.
30. W. Denk *et al.* (1990) *Science* **248**, 73–76.
31. C. J. R. Sheppard and M. Gu (1990) *Optik* **86**, 104–106.
32. C. Xu *et al.* (1996) *Bioimaging* **4**, 198–207.
33. K. König *et al.* (2000) *Single Mol.* **1**, 41–51.

34. T. P. Stauffer and T. Meyer (1997) *J. Cell Biol.* **139**, 1447–1454.
35. I. Parolini *et al.* (1999) *J. Biol. Chem.* **20**, 14176–14187.
36. P.-O. Vidalain *et al.* (2000) *EMBO J.* **19**, 3304–3313.
37. S. Mañes *et al.* (1999) *EMBO J.* **18**, 6211–6220.
38. M. Kawabuchi *et al.* (2000) *Nature* **404**, 999–1003.
39. C. A. Baumann *et al.* (2000) *Nature* **407**, 202–207.
40. K. Röper *et al.* (2000) *Nature Cell Biol.* **2**, 582–592.
41. A. Viola *et al.* (1999) *Science* **283**, 680–682.
42. C. R. F. Monks *et al.* (1998) *Nature* **395**, 82–86.
43. P. Verkade *et al.* (2000) *J. Cell Biol.* **148**, 727–739.
44. P. W. Janes *et al.* (1999) *J. Cell Biol.* **147**, 447–461.
45. R. H. Webb and C. K. Dorey (1995) in J. B. Pawley (Ed.), *Handbook of Biolocical Confocal Microscopy, Plenum Press*, New York, pp. 55–67.
46. M. Petrán *et al.* (1968) *J. Opt. Soc. Am.* **58**, 661–664.
47. R. Juškaitis *et al.* (1996) *Nature* **383**, 804–806.
48. J. Bewersdorf *et al.* (1998) *Opt. Lett.* **23**, 655–657.
49. Th. Förster (1948) *Ann. Phys.* **6**, 55–57.
50. A. Jenei *et al.* (1997) *Proc. Natl. Acad. Sci. USA* **94**, 7269–7274.
51. A. Götz *et al.* (submitted for publication).
52. A. K. Kenworthy and M. Edidin (1998) *J. Cell Biol.* **142**, 69–84.
53. R. Varma and S. Mayor (1998) *Nature* **394**, 798–801.
54. R. C. Dunn (1999) *Chem. Rev.* **99**, 2891–2927.
55. N. F. van Hulst *et al.* (1997) *J. Struct. Biol.* **119**, 222–231.
56. Th. Enderle *et al.* (1998) *Ultramicroscopy* **71**, 303–309.
57. J. Hwang *et al.* (1998) *Biophys. J.* **74**, 2184–2190.
58. Th. Enderle *et al.* (1997) *Proc. Natl. Acad. Sci. USA* **94**, 520–525.
59. L. S. Barak and W. W. Webb (1981) *J. Cell Biol.* **90**, 595–604.
60. M. Saxton and K. Jacobson (1997) *Annu. Rev. Biophys. Biomol. Struct.* **26**, 373–399.
61. J. Gelles *et al.* (1988) *Nature* **331**, 450–454.
62. C. M. Anderson *et al.* (1992) *J. Cell. Sci.* **101**, 415–425.
63. A. Kusumi *et al.* (1993) *Biophys. J.* **65**, 2021–2040.
64. R. Ghosh and W. W. Webb (1994) *Biophys. J.* **66**, 1301–1318.
65. Y. Sako and A. Kusumi (1994) *J. Cell Biol.* **125**, 1251–1264.
66. R. Simson *et al.* (1995) *Biophys. J.* **69**, 989–993.
67. E. D. Sheets *et al.* (1997) *Biochemistry* **36**, 12449–12458.
68. R. Simson *et al.* (1998) *Biophys. J.* **74**, 297–309.
69. D. Gross and W. W. Webb (1986) *Biophys. J.* **49**, 901–911.
70. H. Geerts *et al.* (1987) *Biophys. J.* **52**, 775–782.
71. M. Edidin *et al.* (1991) *Science* **254**, 1379–1382.
72. G. M. Lee *et al.* (1991) *Proc. Natl. Acad. Sci. USA* **88**, 6274–6278.
73. M. Fein *et al.* (1993) *J. Membrane Biol.* **135**, 83–92.
74. M. Tomishige *et al.* (1998) *J. Cell Biol.* **142**, 989–1000.
75. Y. Sako *et al.* (1998) *J. Cell Biol.* **140**, 1227–1240.
76. M. J. Saxton (1995) *Biophys. J.* **69**, 389–398.
77. F. Zhang *et al.* (1993) *Bioessays* **15**, 579–588.
78. V. T. Oi *et al.* (1982) *J. Cell Biol.* **93**, 981–986.
79. K. Peck *et al.* (1989) *Proc. Natl. Acad. Sci. USA* **86**, 4087–4091.
80. R. J. Cherry *et al.* (1998) *J. Cell Biol.* **140**, 71–79.
81. P. R. Smith *et al.* (1999) *Biophys. J.* **76**, 3331–3344.
82. M. Bruchez Jr. *et al.* (1998) *Science* **281**, 2013–2016.
83. W. C. W. Chan and S. Nie (1998) *Science* **281**, 2016–2018.
84. Th. Schmidt *et al.* (1999) *Microsc. Res. Tech.* **44**, 339–346.
85. G. J. Schütz *et al.* (2000) *Mol. Membr. Biol.* **17**, 17–29.
86. Th. Schmidt *et al.* (1996) *Proc. Natl. Acad. Sci. USA* **93**, 2926–2929.
87. Th. Schmidt *et al.* (1996) *Anal. Chem.* **68**, 4397–4401.
88. G. J. Schütz *et al.* (1997) *Opt. Lett.* **22**, 651–653.
89. G. S. Harms *et al.* (1999) *Biophys. J.* **77**, 2864–2870.
90. G. J. Schütz *et al.* (1998) *Biophys. J.* **74**, 2223–2226.
91. S. Chandrasekhar (1943) *Rev. Mod. Phys.* **15**, 1–89.
92. J. E. Aubin (1979) *J. Histochem. Cytochem.* **27**, 36–43.
93. R. C. Benson *et al.* (1979) *J. Histochem. Cytochem.* **27**, 44–48.
94. J. Marelius (1995) M.Sc. thesis, Uppsala University, Uppsala, Sweden.
95. G. J. Schütz (2000) *Single Mol.* **1**, 25–31.
96. Y. Sako *et al.* (2000) *Nature Cell Biol.* **2**, 168–172.
97. T. A. Byassee *et al.* (2000) *Anal. Chem.* **72**, 5606–5611.
98. B. R. Masters *et al.* (1997) *Biophys. J.* **72**, 2405–2412.
99. N. Bobroff (1986) *Rev. Sci. Instrum.* **57**, 1152–1157.
100. C. Eggeling *et al.* (1998) *Anal. Chem.* **70**, 2651–2659.
101. B. Wilson *et al.* (2000) *J. Cell Biol.* **149**, 1131–1142.
102. J. E. Schnitzer *et al.* (1995) *Science* **269**, 1435–1439.
103. H. X. You and L. Yu (1999) *Methods Cell Sci.* **21**, 1–17.
104. V. Vie *et al.* (2000) *Ultramicroscopy* **82**, 279–288.
105. G. U. Lee *et al.* (1994) *Langmuir* **10**, 354–357.
106. P. Hinterdorfer *et al.* (1996) *Proc. Natl. Acad. Sci. USA* **93**, 3477–3481.
107. P. P. Lehenkari and M. A. Horton (1999) *Biochem. Biophys. Res. Commun.* **259**, 645–650.
108. A. Chen and V. T. Moy (2000) *Biophys. J.* **78**, 2814–2820.
109. C. Yuan and L. J. Johnston (2000) *Biophys. J.* **79**, 2768–2781.
110. M.-C. Giocondi *et al.* (2000) *J. Struct. Biol.* **131**, 38–43.
111. M. B. Viani *et al.* (2000) *Nature Struct. Biol.* **7**, 644–647.
112. M. Pitto *et al.* (1999) *Biochem. J.* **344**, 177–184.
113. A. Pralle *et al.* (2000) *J. Cell Biol.* **148**, 997–1007.
114. K. Simons and D. Toomre (2000) *Nature Rev. Mol. Cell Biol.* **1**, 31–39.
115. K. Jacobson and C. Dietrich (1999) *Trends Cell Biol.* **9**, 87–91.